Journal of Biomedical Optics

BiomedicalOptics.SPIEDigitalLibrary.org

Optical tracer size differences allow quantitation of active pumping rate versus Stokes–Einstein diffusion in lymphatic transport

Alisha V. DSouza
Kayla Marra
Jason R. Gunn
Kimberley S. Samkoe
Brian W. Pogue

SPIE.

Alisha V. DSouza, Kayla Marra, Jason R. Gunn, Kimberley S. Samkoe, Brian W. Pogue, "Optical tracer size differences allow quantitation of active pumping rate versus Stokes–Einstein diffusion in lymphatic transport," *J. Biomed. Opt.* **21**(10), 100501 (2016), doi: 10.1117/1.JBO.21.10.100501.

Optical tracer size differences allow quantitation of active pumping rate versus Stokes–Einstein diffusion in lymphatic transport

Alisha V. DSouza,[a,*] Kayla Marra,[a] Jason R. Gunn,[a] Kimberley S. Samkoe,[a,b] and Brian W. Pogue[a,b,*]
[a]Dartmouth College, Thayer School of Engineering, 14 Engineering Drive, Hanover, New Hampshire 03755, United States
[b]Geisel School of Medicine, Department of Surgery, 1 Rope Ferry Road, Hanover, New Hampshire 03755, United States

Abstract. Lymphatic uptake of interstitially administered agents occurs by passive convective–diffusive inflow driven by interstitial concentration and pressure, while the downstream lymphatic transport is facilitated by active propulsive contractions of lymphatic vessel walls. Near-infrared fluorescence imaging in mice was used to measure these central components of lymphatic transport for the first time, using two different-sized molecules—methylene blue (MB) and fluorescence-labeled antibody immunoglobulin G (IgG)-IRDye 680RD. This work confirms the hypothesis that lymphatic passive inflow and active propulsion rates can be separated based upon the relative differences in Stokes–Einstein diffusion coefficient. This coefficient specifically affects the passive-diffusive uptake when the interstitial volume and pressure are constant. Parameters such as mean time-to-peak signal, overall fluorescence signal intensities, and number of active peristaltic pulses, were estimated from temporal imaging data. While the mean time to attain peak signal representative of diffusion-dominated flow in the lymph vessels was 0.6 ± 0.2 min for MB and 8 ± 6 min for IgG, showing a size dependence, the active propulsion rates were 3.4 ± 0.8 pulses/min and 3.3 ± 0.5 pulses/min, respectively, appearing size independent. The propulsion rates for both dyes decreased with clearance from the interstitial injection-site, indicating intrinsic control of the smooth muscles in response to interstitial pressure. This approach to size-comparative agent flow imaging of lymphatic function can enable noninvasive characterization of diseases related to uptake and flow in lymph networks. [DOI: 10.1117/1.JBO.21.10.100501]

Keywords: lymphatics; fluorescence; imaging; pharmacokinetics.

Paper 160527LR received Aug. 2, 2016; accepted for publication Sep. 20, 2016; published online Oct. 18, 2016.

*Address all correspondence to: Alisha V. DSouza, E-mail: Alisha.V.Dsouza@dartmouth.edu; Brian W. Pogue, E-mail: brian.w.pogue@dartmouth.edu

The lymphatic system provides the central channel for interstitial fluid flow, dissemination of immune cells, molecular response to pathogens,[1] cancers metastases,[2] and potential for drug delivery.[3] This system functions without an internal pump and net lymph flow has contributions from the rate of lymph formation and solute uptake at the interstitium, and lymph propulsion. Lymph formation and solute uptake are predominantly driven by convection and diffusion into the lymphatic capillaries in the interstitial space;[4] on the other hand, skeletal muscle movements, blood pressure, and phasic smooth muscle contractions of the collector lymph vessels induce the pressure for propelling lymph along the vessel length.[5] Interstitial administration of imaging tracers[6] has implications in a range of disease conditions, such as metastatic cancers of the skin, breast, abdomen, and head for diagnostic staging.[7] Yet, while this imaging is critically important for the majority of surgical oncology procedures, there have been few attempts to quantitatively visualize and study the lymphatic system,[8–10] and extract possible parametric values for assessment of function[10] and disease status.[11] Most studies have focused on relative observations of intensity, yet there is good potential for making decisions based on quantitative parametric information derived from imaging lymph nodes[12] and lymphatic vessels.[13] Herein, we hypothesized that by imaging lymphatic flow of two different sized tracers, the relative contributions of propulsive flow and the convective–diffusive interstitial solute uptake could be separated and quantified.

Wide-field near-infrared fluorescence (NIRF) imaging and intravital microscopy are two of the most common methods applied in mechanistic studies of the lymphatics *in vivo* with the former showing promise for imaging human subjects as well as small animals,[14] and the latter applied to finding basic mechanisms. NIRF methods also offer the benefit of high temporal resolution and simultaneous multiagent imaging.[15] However, drug and dye delivery via the lymphatics suffers from issues of high heterogeneity, and intensity-based metrics often need to be considered carefully with appropriate correction for delivery differences.[16] An understanding of tracer lymphatic pharmacokinetics and the influencing factors is also essential for designing appropriate imaging studies and protocols. For example, Aldrich et al.[17] compared the effects of varying concentration of indocyanine green on the lymphatic propulsion, and Wu et al.[18] compared the uptake of albumin-bound versusfree IRDye 680RD from mouse paw by axillary nodes. Lymphatic flow in the vessels is driven by diffusion and convection at the interstitium, and the lymphatic contractions of the smooth muscles lining the collector lymph vessels induce the periodic pressure gradients to maintain lymph flow. Valves present along each lymph vessel prevent retrograde flow, and the rhythmic smooth muscle contractions propel lymph from one lymph vessel segment (lymphangion) to the next.[5] Bulk fluid flow at the interstitium into lymph capillaries is dominated by the pressure-driven flow induced by the injected fluid volume, and the influx of tracer molecules is dominated by diffusion. The molecular size, shape, charge, and affinity to proteins in the lymph can each influence the transport of solute molecules at the injection size into the lymphatics and, hence, affect the overall tracer kinetics, yet the lymph formation and propulsion processes are affected differently by these factors. The goal of this work was to quantitatively characterize the lymphatic uptake and transport of a large nonspecific antibody tracer [i.e., immunoglobulin G (IgG)], as compared to small

dye molecules [i.e., methylene blue (MB)] approved for interstitial lymphatic administration,[19] and extract parametric values of the influence of molecule size upon the pharmacokinetics of lymphatic transport. To the best of our knowledge, this is the first quantitative study of active transport and passive uptake mechanisms in the normal lymphatics for comparing large and small tracers in the same animals.

Specifically, the difference in transport of MB (molecular weight ~300 Da), which may weakly and reversibly associate with protein albumin (molecular weight ~66.5 kDa) in the lymph (association constant, $K_a = 4.012 \times 10^4$ M^{-1} at 298 K[20]), was analyzed and compared to the larger mouse IgG conjugated to fluorophore (size >150 kDa). We defined the "active propulsion" component as the flow of fluorescence dye molecules from one lymphangion to the next, i.e., peristalsis, as identified by the number of contractions and relaxations of the lymph vessel. The overall transport of tracers through the lymphatics is a combination of this active component and a passive diffusion- and interstitial pressure-driven uptake component at the interstitium, which for simplicity is referred to as the "passive uptake." We documented the action of tracers in both the active and passive components of flow through the collector lymphatic vessels[4,5] when injection volume was fixed for both tracers, thus eliminating any relative effects of pressure gradient in the interstitium. The small size of MB, combined with its low affinity for albumin in lymph,[21] makes its movement through the lymphatic system very swift.

The antibody tracer used was mouse IgG (Athens Research and Technology, Athens, Georgia) Isotype control antibody for Erbitux labeled with IRDye 680RD (LI-COR Biosciences, Lincoln, Nebraska). The labeling procedures for the former are described in detail in previous work.[7] The IgG-labeled solution was concentrated to μM concentrations. The MB (NDC 17478-504-10, Akorn Inc.) was diluted in phosphate-buffered saline (PBS) to a concentration of ~2.5 mM.

All animal experiments were carried out in accordance with the Institutional Animal Care and Use Committee at Dartmouth College under approved protocols. A total of 13, 8- to 10-week-old athymic nude female mice (Charles River, Wilmington, Massachusetts) were used in this study. Animals were grouped into two cohorts—MB-injected and mouse IgG-IRDye-injected. All animals were maintained on a fluorescence-free diet for a week prior to imaging. Prior to imaging, each animal was anaesthetized using 1.5% to 3% isofluorane (Piramal, Bethlehem, Pennsylvania) in 1.5 L/min oxygen. It was then placed on its side with the forelimb on one side of the body stretched out so as to expose lymph nodes of the axilla, as shown in Fig. 1. A preinjection image was captured to measure autofluorescence background levels. The IgG-IRDye tracer was diluted in PBS so that 10 μl contained 0.1 nmoles of protein. 10-μl volume of each fluorescent tracer in PBS was injected intradermally using a 31-gauge syringe needle into the base of a forepaw of each animal. All fluorescence imaging was performed using a Pearl® Impulse system (LI-COR Biosciences Inc., Lincoln, Nebraska), which provides planar surface images in two near-infrared bands.[22] The system was set up to acquire 700-nm channel images at 1 frame every 2 s for the first 10 to 20 min, and then at 2 frames per minute. Imaging was performed for 120 min following injection.

Image analysis was performed using MATLAB® (R2014b, Mathworks, Natick, Massachusetts) and Image J Software [1.47 v, National Institutes of Health (NIH)]. Regions of interest (ROIs) were selected over the visible lymph node and its afferent lymphatic vessel. For nodes, circular ROIs of 2020-μm diameter were drawn, and for lymphatic vessels, three ROIs each ~500 μm in diameter were selected over different sections of the collector lymphatics. Care was taken to place the ROIs over regions where there was evidence of pumping function. We expected to see sections with a lack of pumping function along each vessel; these regions were avoided for the purpose of this study. Fluorescence signal at various time points after tracer administration was observed. Statistical analyses were performed using Microsoft Excel, assuming equal variances across all groups. A student's t-test was used to identify parameters with significant differences between the MB and IgG cohorts.

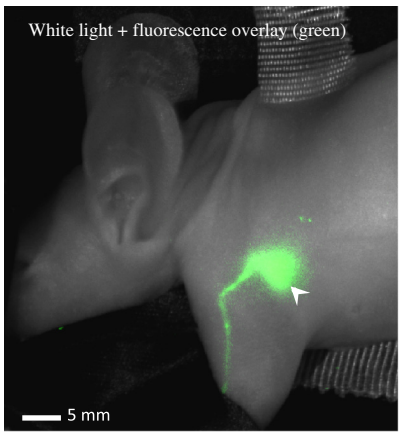

Fig. 1 Uptake of MB from the injection site in the paw to an axillary lymph node (white arrow).

Figure 1 shows the uptake of MB from an injection site in a mouse paw to the axillary lymph node. The paw had to be covered to block out the large fluorescence signal from the deposited dye. The transport of tracer appeared to have both an active pumping and a passive diffusion- and pressure-driven component as expected.[4] A sample set of measured MB uptake curves in one mouse is shown in Fig. 2. The overall uptake shapes were recovered using temporal smoothing with piecewise spline fitting with a smoothing resolution of 18 s, and the dotted lines represent the previously defined "passive uptake." Based on the fluorescence intensity signal strength, only one vessel segment was chosen for analysis in each animal. This was generally the vessel segment close to the lymph node, as signal-to-noise was poor at segments close to the paw. Periodic vessel contractions were evident in the raw fluorescence measurements, and signal troughs could be manually counted to identify number of pulses per unit time. Due to the noise in the data, relative intensities of pulses, to each other and to the overall uptake, were not estimated. The number of pulses per unit time was used to describe the "active propulsion." The early time points where tracer is rapidly taken into the lymph vessels were called the "transient" phase, and the later time points where dye fluorescence steadily declines are the "steady-state" phase as it can be used to estimate the resting contractile lymphatic propulsion. For MB, the transient phase lasted between ~0 and 2 min, and for IgG-IRDye, it was ~0 to 15 min.

Figure 3 shows a representative set of overall uptake curves for MB and mouse IgG-IRDye in the axillary node and a corresponding afferent lymph vessel segment at a location ~5 mm to the node. The curves were normalized to the peak fluorescence signal in the vessel. IgG accumulation peaks at ~60 min

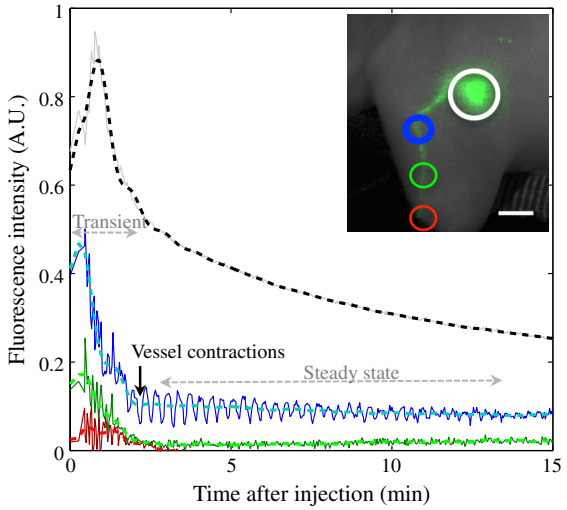

Fig. 2 Active and passive components of lymphatic uptake of MB. Inset shows representative ROI locations (circles were enlarged to be visible, actual ROI size was ~2 mm for nodes and 0.5 mm for lymph vessels). ROI circles are color coded to match the uptake curves. Raw data (light solid lines) and smoothed curves (dotted lines) are shown. 5-mm scale bar is shown on inset.

in the lymph node and MB peaks at ~1 min. The peak fluorescence is attained in the vessel segment much earlier than in the node. The MB vessel peak, is missed in these presented data from one animal, owing to the fact that it can get taken up during injection itself and is instantaneously driven forward. MB is not retained within the lymph node and clears immediately, whereas IgG, owing to its large size, remains in the lymph node for a significantly longer time.

The time to reach the peak fluorescence in the node, $T_{\text{peak},N}$ was noted for all animals and found to be 0.8 ± 0.4 min (median $\pm$ standard deviation, excluding outliers beyond $\pm 2\sigma$), in the MB group, and 65 ± 23 min in the IgG-IRDye group. Similarly, time to peak in the vessel $T_{\text{peak},V}$ was observed to be 0.6 ± 0.2 min and 8 ± 6 min in the MB and IgG-IRDye groups, respectively [see Figs. 4(a) and 4(b)]. The differences between these groups were found to be significant with p value ≈ 0 for nodes and p value $= 0.008$ in the vessels. We have previously shown that raw intensity measurements

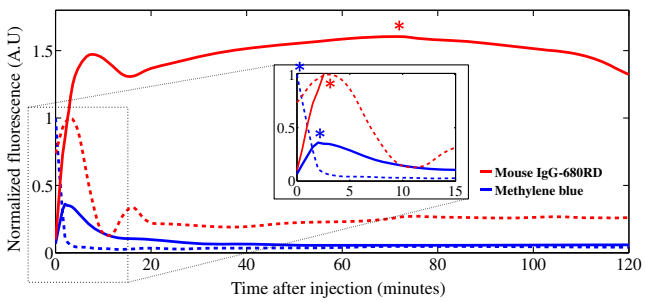

Fig. 3 Comparison of passive uptake components of MB and IgG-IRDye shown in a representative lymph node (solid) and its corresponding afferent lymph vessel (dotted). MB clears rapidly from the node owing to its small size. Inset shows a time-expanded view. Note that curves were smoothed, so active lymph vessel propulsion is not evident here. The second peak (indicated by red asterisk in the main plot) of the double peak seen in the IgG-IRDye uptake in the lymph node was always found to be higher in signal intensity that the first and was chosen for peak time and intensity estimation. Color-coded asterisks have been used to indicate peak locations.

on the nodes are highly unreliable and prone to high-signal heterogeneity, attributable to heterogeneity in delivery by the lymphatic vessel,[16] and so vessel signal-based normalization improves the quantification of signal in the nodes provided that a single vessel delivers tracer, and tracer has not entered the blood stream. We report vessel-peak normalized node fluorescence N/V in Fig. 4(c) and found that this ratio was 1.7 ± 0.8 in the MB group and 7 ± 4 in the IgG-IRDye group, revealing a statistically significant difference between groups with p value $= 0.004$. All the above parameters are related to the slower rate of uptake of IgG-IRDye as compared to the much smaller MB molecule at the lymphatic–interstitial interface. If this flow was purely diffusive their relative transport times would be dominated by the Stokes–Einstein diffusion coefficient D, ($D = kT/6\pi\eta r$) (where k is the Bolztmann constant, T is the temperature, η is the viscocity, and r is the particle radius). Given the relative sizes, $r \sim (\text{MW})^{1/3}$, of the MB to IgG, their relative diffusion coefficients would be a ratio of 1:7.9. This ratio is interstingly very close to the measured ratio of time to peak [see Fig. 4(b)], 0.6:8, in the afferent vessels, and within the error bounds of the estimates, indicating that diffusive transport dominates this slower passive uptake process, although the ratio in the nodes appears further from this, at 0.8:65, likely due to differing kinetics of tracer exiting the nodes to downstream lymphatics and vasculature, a discussion of which is beyond the scope of this work. The above indicates that as long as the injected agent volume is constant and hence interstitial pressure is constant, diffusion dominates the uptake of molecules into the lymphatic capillaries.

The lymph nodes, being clearance organs, retain large proteins and molecules, and hence, the tracer lymphatic kinetics is influenced by this retention. MB appears to be barely retained by the node and is seen in the urine within minutes after injection (data not shown). Other studies suggest that MB has very poor affinity for any plasma proteins due to the lack of sulphonic acid groups,[21] and hence mostly exists as free unassociated dye that can travel swiftly into and out of the node. IgG-IRDye on the other hand is likely trapped in the lymph node sinuses and clears slowly after injection.

Figures 4(d) and 4(e) show the intensity independent-"active" propulsive components of the transport. Contractions of smooth muscles lining the walls of the collector lymph vessels drive the lymph packets from one lymphangion to the next. The number of complete pulses per minute was counted from the raw fluorescence data as shown in Fig. 2. The early time points during which tracer signal in the node and lymph vessel were rapidly changing (~0 to 2 min for MB and ~0 to 15 min for IgG) was labeled "Transient pump rate, p_{trans}" and the pump rate over late time points was assumed to be indicative of the resting pump rate and was labeled, "steady-state pump rate, p_{∞}." We estimated the time windows based upon the $T_{\text{peak},V}$ median values, which were 0.6 and 8 min for MB and IgG, respectively. We approximated that "steady state" time would exist after about twice this duration across all animals, and that the uptake from the 0-min time point to the $2 \times T_{\text{peak},V}$ time point would be "transient state." For the MB and IgG cohorts, transient pump rates were observed to be 6.1 ± 1.3 and 4.2 ± 1.2 pulses/min (p value $= 0.15$), and steady-state pump rates were 3.4 ± 0.8 and 3.3 ± 0.5 pulses/min (p value $= 0.34$). The pump rates were similar for the MB and IgG cohorts indicating that molecule size does not affect the propulsion rate due to lymphatic vessel contractions. Aldrich et al.[17] observed similar pumping

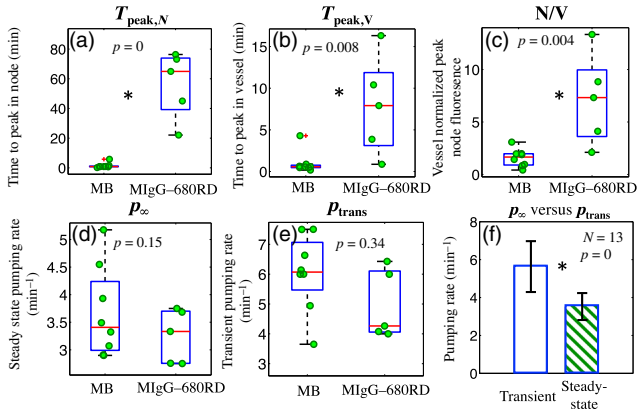

Fig. 4 (a)–(e) Comparison of various measured parameters for MB ($N = 8$) and MIgG-IRDye 680RD ($N = 5$) cohorts. (f) shows comparison bar graphs of transient versus steady-state propulsion rate in all animals. * indicates significant difference with p value < 0.009.

(propulsion) rates in their comparison of indocyanine green, IRDye 800CW, and an antibody, though they did not separate transient and steady-state rates, and instead used the average rate over 20 min. Given that there was no significant differences in pump rates between the MB and IgG cohorts, we pooled the results from both cohorts and compared the transient (6.0 ± 1.4 pulses/min) and steady-state rate (3.4 ± 0.8 pulses/min) within each mouse using a paired-student's t-test and found that the differences were significant with p value ≈ 0, indicating that the collector lymphatics likely do respond to luminal pressure changes in the initial lymphatic capillaries.[23] While we expect that there are differences in the intersititial oncotic pressure due to IgG versus MB, the hydrostatic pressure is likely dominant (due to large injection volume of 10 μl) preventing differences between MB and IgG to be significant in influencing interstitial pressure. Also, note that no detectable contraction was observed in the lymph nodes.

The study of the lymphatic physiology has largely been limited by the inability to image the lymphatic architecture in real time at a sampling rate greater than the lymphatic smooth muscle contraction rate. Recent attempts using near-infrared and far-red fluorophores, and imaging using microscopy methods, such as intravital microscopy[9] and broad-beam NIRF imaging,[10] have lead the way in quantitative imaging of lymphatic vessels but so far do not describe the relationship between tracer size and various components of transport. Through this work we quantitatively studied and compared active propulsion and passive uptake in the lymphatics for large and small tracers and hope to elucidate the importance of identifying these components of transport; we expect that this work will be one piece in the puzzle of developing the right tools to study the lymphatic vasculature and use appropriate physiological models, which will in turn impact the ability to better diagnose lymphatic diseases, such as metastasis, noninvasively.

Acknowledgments

This work was supported by the NIH Grant No. R01 CA109558 and the U.S. Army Medical Research and Material Command Grant No. W81XWH-16-1-0004 from the Congressionally Directed Medical Research Program on Breast Cancer.

References

1. J.-P. Girard, C. Moussion, and R. Forster, "HEVs, lymphatics and homeostatic immune cell trafficking in lymph nodes," *Nat. Rev. Immunol.* **12**(11), 762–773 (2012).
2. T. P. Padera et al., "Lymphatic metastasis in the absence of functional intratumor lymphatics," *Science* **296**(5574), 1883–1886 (2002).
3. S. Cai et al., "Lymphatic drug delivery using engineered liposomes and solid lipid nanoparticles," *Adv. Drug Delivery Rev.* **63**(10–11), 901–908 (2011).
4. H. Wiig and M. A. Swartz, "Interstitial fluid and lymph formation and transport: physiological regulation and roles in inflammation and cancer," *Physiol. Rev.* **92**(3), 1005–1060 (2012).
5. G. W. Schmid-Schonbein, "Microlymphatics and lymph flow," *Physiol. Rev.* **70**(4), 987–1028 (1990).
6. N. K. Tafreshi et al., "A mammaglobin-A targeting agent for noninvasive detection of breast cancer metastasis in lymph nodes," *Cancer Res.* **71**(3), 1050–1059 (2011).
7. K. M. Tichauer et al., "Microscopic lymph node tumor burden quantified by macroscopic dual-tracer molecular imaging," *Nat. Med.* **20**(11), 1348–1353 (2014).
8. H. S. Tran Cao et al., "Imaging of the interaction of cancer cells and the lymphatic system," *Adv. Drug Delivery Rev.* **63**(10–11), 886–889 (2011).
9. S. Liao et al., "Method for the quantitative measurement of collecting lymphatic vessel contraction in mice," *J. Biol. Methods* **1**(2), e6 (2014).
10. S. Kwon and E. M. Sevick-Muraca, "Noninvasive quantitative imaging of lymph function in mice," *Lymphatic Res. Biol.* **5**(4), 219–231 (2007).
11. R. Sharma et al., "Quantitative imaging of lymph function," *Am. J. Physiol. Heart Circ. Physiol.* **292**(6), H3109–H3118 (2007).
12. N. K. Tafreshi et al., "Noninvasive detection of breast cancer lymph node metastasis using carbonic anhydrases IX and XII targeted imaging probes," *Clin. Cancer Res.* **18**(1), 207–219 (2012).
13. S. Kwon et al., "Direct visualization of changes of lymphatic function and drainage pathways in lymph node metastasis of B16F10 melanoma using near-infrared fluorescence imaging," *Biomed. Opt. Express* **4**(6), 967–977 (2013).
14. J. C. Rasmussen, C. E. Fife, and E. M. Sevick-Muraca, "Near-infrared fluorescence lymphatic imaging in lymphangiomatosis," *Lymphatic Res. Biol.* **13**(3), 195–201 (2015).
15. A. V. DSouza et al., "Review of fluorescence guided surgery systems: identification of key performance capabilities beyond indocyanine green imaging," *J. Biomed. Opt.* **21**(8), 080901 (2016).
16. A. V. DSouza et al., "Nodal lymph flow quantified with afferent vessel input function allows differentiation between normal and cancer-bearing nodes," *Biomed. Opt. Express* **6**(4), 1304–1317 (2015).
17. M. B. Aldrich et al., "Concentration of indocyanine green does not significantly influence lymphatic function as assessed by near-infrared imaging," *Lymphatic Res. Biol.* **10**(1), 20–24 (2012).
18. F. Wu et al., "Noninvasive real-time fluorescence imaging of the lymphatic uptake of BSA-IRDye 680 conjugate administered subcutaneously in mice," *J. Pharm. Sci.* **101**(5), 1744–1754 (2012).
19. R. Simmons et al., "Methylene blue dye as an alternative to isosulfan blue dye for sentinel lymph node localization," *Ann. Surg. Oncol.* **10**(3), 242–247 (2003).
20. L. L. He et al., "Enhancement of the binding affinity of methylene blue to site I in human serum albumin by cupric and ferric ions," *Luminescence* **30**(8), 1380–1388 (2015).
21. C. Tsopelas and R. Sutton, "Why certain dyes are useful for localizing the sentinel lymph node," *J. Nucl. Med.* **43**(10), 1377–1382 (2002).
22. C. J. Lesiak, A. Bouzid, and D. Franzen, "Wide dynamic range imaging," Google Patent Number: 8,743,241 B2 (2014).
23. W. L. Olszewski and A. Engeset, "Intrinsic contractility of prenodal lymph vessels and lymph flow in human leg," *Am. J. Physiol.* **239**(6), H775–H783 (1980).